A numerical framework for modeling fate and transport of microplastics in inland and coastal waters

Abolghasem Pilechi [*], Abdolmajid Mohammadian, Enda Murphy

Ocean, Coastal & River Engineering Research Centre, National Research Council Canada, Ottawa, Canada
Department of Civil Engineering, University of Ottawa, Ottawa, Canada

ABSTRACT

Proliferation of microplastics in rivers, lakes, estuaries, coastal waters and oceans is a major global challenge and threat to the environment, livelihoods and human health. Reliable predictive tools can play an essential role in developing an improved understanding of microplastics behaviour, exposure and risk in water bodies, and facilitate identification of sources and accumulation hot spots, thereby enabling informed decision-making for targeted prevention and clean-up activities. This study presents a new numerical framework (CaMPSim-3D) for predicting microplastics fate and transport in different aquatic settings, which consists of a Lagrangian, three-dimensional (3D) particle-tracking model (PTM) coupled with an Eulerian-based hydrodynamic modeling system (TELEMAC). The 3D PTM has several innovative features that enable accurate simulation and efficient coupling with TELEMAC, which utilizes an unstructured computational mesh. The PTM is capable of considering spatio-temporally varying diffusivity, and uses an innovative algorithm to locate particles within the Eulerian mesh. Model accuracy associated with different advection schemes was verified by comparing numerical predictions to known analytical solutions for several test cases. The implications of choosing different advection schemes for modeling microplastics transport was then investigated by applying the PTM to simulate particle transport in the lower Saint John River Estuary in eastern Canada. The sensitivity of the PTM predictions to the advection scheme was investigated using six numerical schemes with different levels of complexity. Predicted particle distributions and residence times based on the fourth-order Runge–Kutta (RK4) scheme differed significantly (residence times by up to 100 %) from those computed using the traditional first-order (Euler) method. The Third Order Total Variation Diminishing (TVD3) Runge-Kutta method was found to be optimal, providing the closest results to RK4 with approximately 27 % lower computational cost.

1. Introduction

Microplastics and their impacts on the aquatic environment and human life have received significant attention from governments, water resources managers, environmental regulators and the general public over the last decade (Hüffer et al., 2017a). Microplastics are generally defined as any plastic particles with characteristic length scales <5 mm (Andrady, 2011; Cole et al., 2011; Costa et al., 2011; Lee et al., 2013; Besseling et al., 2017; Wright et al., 2018). These particles are small enough to be ingested by aquatic organisms and subsequently proceed along the marine food web to the human body. Moreover, due to their large surface area-to-volume ratio and high mobility, microplastics have high potential for absorbing and dispersing different types of contaminants, organic matter, and invasive species (Rios et al., 2007; Betts,

2008; Ashton et al., 2010; Koelmans et al., 2013; Lo et al., 2018; Caruso, 2019). Microplastics derive from different compounds, characterized by different densities. Nine of the main polymer types found in marine environments, and their densities, are listed in Table 1 (Andrady, 2011). Microplastics can also be classified based on particle shapes or geometries, which can include spheres, granules, films, and fibres (Van Melkebeke et al., 2020).

Understanding fate and transport of microplastics in water is a key focus area for research (Hardesty et al., 2017; Hüffer et al., 2017b). As a mass-transport problem in a fluid medium, the movement and transformation of microplastics in water can be described by the advection-diffusion-reaction (Eq. 1),

$$\frac{\partial S}{\partial t} = \nabla \bullet (SU) + \nabla \bullet (K\nabla SU) + \rho(S) \tag{1}$$

Table 1

Densities of microplastic particles commonly found in the environment (adapted from Andrady, 2011).

Type	Density (kg/m^3)
Polyethylene (PE)	910–950
Polypropylene (PP)	900–920
Polystyrene (expanded)	1–1050
Polystyrene (PS)	1040–1090
Poly vinyl chloride (PVC)	1160–1300
Polyamide (PA) or nylon	1130–1150
Polyethylene terephthalate (PET)	1340–1390
Polyester resin + glass fibre	>1350
Cellulose acetate	1220–1240

where S is the concentration, K is the diffusion coefficient, U is the velocity of the ambient environment, t is the time and $\rho(S)$ is the reaction function. Diffusion is the process whereby particles spread due to molecular (Brownian) motion and turbulence. Dispersion, spreading associated with the combined effects of velocity gradients and diffusion, is often approximated as a diffusive process.

Computer models that can provide reliable predictions of the movement and behaviour of microplastic particles in water are potentially valuable tools for identifying accumulation hot spots, pathways and potential sources, and ultimately guiding clean-up/recovery activities. Predictive models can also help to promote awareness and support education, decision-making, and policy development surrounding prevention, mitigation and remediation activities. Lagrangian models, also known as particle-tracking models (PTMs), are a class of numerical models that can be used to predict the movement of discrete particles or objects in various media, such as air or water. At each time step, the position and motion of particles is determined by solving governing transport equations in a reference frame that moves with the particles. Particles can either be considered as passive objects that follow the ambient flow field (i.e., kinematic approach), or their movement can be determined based on the balance of forces (e.g., gravity, friction, drag, inertia) and interactions between the particles and the medium in which they reside (i.e., dynamic approach). In the dynamic approach, particles are driven by the resultant applicable external/internal forces on them, based on the equation of motion.

At each time step of simulation with PTMs, transport equations are only solved for the active (e.g. in motion) particles in the domain. Whereas, in Eulerian models the governing equations are solved for all of the computational cells during simulation. For a similar total number of particles and computational nodes, Hunter (1987) showed that particle-tracking technique is significantly more efficient than conventional finite-difference methods in higher-dimension cases, or when the particles patch occupies only a portion of the whole model domain (heterogeneously-distributed). PTMs normally have higher computational stability than explicit Eulerian models permitting them to use larger time steps while maintaining accuracy (Staniforth and Cote, 1991; Neuman, 1984). They also allow for accurate simulation of non-diffusive transport in high Peclet-number (advection-dominated) flows. This feature is of particular importance in the cases where the gradient of concentration is steep (Neuman, 1984; Hunter, 1987; Szymczak and Ladd, 2003). PTMs are also more compatible with the nature of parallel computation parallel computation which can significantly enhance the computational speed (Dimou and Adams, 1993). PTMs can be conveniently used for analysing integral parameters such as residence time and ages of the particles, which are linked to the transformation processes such as weathering and degradation, and influence microplastics transport in aquatic systems. Contamination sources in PTMs are represented by releasing particles at source locations, and concentrations are calculated based on the number of particles occupying a defined volume at a given time.

Typically, PTMs for simulating pollutant transport in water bodies rely on hydrodynamic inputs (e.g., water levels, velocities, turbulence) from Eulerian models, such as ocean general circulation models (OGCM's) (Potemra, 2012; van Sebille et al., 2018) or other hydrodynamic models (Jalón-Rojas et al., 2019). PTMs relying on Eulerian model inputs are therefore often referred to as hybrid Eulerian-Lagrangian models (Oliveira and Baptista, 1995; Xue et al., 2018). Several Eulerian-Lagrangian numerical tools have been developed for predicting fate and transport of macro-plastics (Mansui et al., 2015; Liubartsevaa et al., 2018; Mansui et al., 2020), oil (North et al., 2011; Goeury et al., 2014; Spaulding, 2017), debris (Bladé and Sánchez-Juny, 2016; Ruiz-Villanueva et al., 2014; Potemra, 2012; Politikos et al., 2017), surface drifters (Kjellsson and Döös, 2012), plankton (Xue et al., 2018), and sediment (Kelsey, 1994) in water systems. Recently, a growing awareness of the potential impacts of microplastics has motivated research and development of models aimed at providing realistic predictions of the behaviour of microplastics in water. Isobe et al. (2014), Iwasakia et al. (2017), Jalón-Rojas et al. (2019), Alosairi et al. (2020), Daily et al. (2020), Soto-Navarro et al. (2020), Mansui et al. (2020), and Mountford and Morales Maqueda (2021) are examples of previous studies where Lagrangian models were used for predicting microplastic debris fate and transport. Hardesty et al. (2017) provides an overview on the application of numerical modeling for simulating fate and transport of microplastics in the marine environment. Isobe et al. (2014) used a vertical two-dimensional (2D) PTM to investigate transport of mesoplastics and microplastics in the near-shore zone of Seto Inland Sea, Japan. Their model was not couple with an Eulerian model for hydrodynamic information, and only accounted for waves (Stocks drift), friction, and buoyancy force for the transport process, which is not realistic (Li et al., 2020). Also, the Isobe et al. (2014) model was 2D vertical and did not allow simulating cross-shore transport of the particles, thus could not capture particles distribution along the shoreline. In a recent Eulerian-Lagrangian modeling study, Mansui et al. (2020) simulated transport of macro (>2 cm) plastic particles near the surface of the Mediterranean Sea using a Lagrangian (PTM) model called ARIANE (Blanke and Raynaud, 1997). The PTM used the surface current velocity field from an oceanic general circulation model (OGCM) to calculate the advection process. Mansui et al.'s model was 2D horizontal (depth-averaged) and forced the particles to remain within 50 cm of the water surface. However, the authors highlighted the need to consider the vertical movement of particles in future model development. Macías et al. (2019) used an Eulerian-Lagrangian model that coupled a General Estuarine Transport Model (GETM) (Burchard and Bolding, 2002) with a PTM (Ichthyop v.3.3) (Leet et al., 2008) to investigate seasonal changes in accumulation patterns of floating litter at the surface of the Mediterranean Sea. The model was 2D horizontal and therefore did not simulate vertical movement of particles within the water column. Soto-Navarro et al. (2020) overcame this limitation by coupling a 3D Ichthyop v.3.3 model with a high resolution circulation model (RCM), which provided 3D current velocity fields in the Mediterranean Sea. However, the model did not consider the impact of vertical diffusivity on particle movement within the water column. In another recent 3D modeling study Jalón-Rojas et al. (2019) developed a three-dimensional PTM, called TrackMPD, to simulate behaviour of microplastic particles in water. The Jalón-Rojas et al. (2019) model improved on previous models in that it includes the capability to incorporate the impact of both particles settling and vertical current to simulate movement of particles within the water column. TrackMPD can be coupled with different OGCMs. The 3D PTMs in Jalón-Rojas et al. (2019) and Soto-Navarro et al. (2020) relied on hydrodynamic input from rectangular (structured) grids only, a limitation for coastal, estuarine, and riverine applications where unstructured grids can provide higher resolution in bays and regions of complex geometry. This means that the models cannot be coupled with hydrodynamic models utilizing the unstructured computational meshes that are needed to adequately resolve hydrodynamics and particulate transport in coastal and inland waters which are characterized by complex morphologies and a variety of relevant spatio-temporal scales. Since human population and activities are concentrated

in and around coastal and inland waters, this is a limiting factor affecting the application of models to better understand human exposure to microplastics and associated impacts. Daily et al. (2020) coupled a three-dimensional PTM model with the Finite Volume Community Ocean Model (FVCOM) to investigate behaviour of different types of microplastics in Lake Erie. FVCOM has the capability to provide hydrodynamic information on an unstructured grid. However, the PTM required hydrodynamic output on a regular grid, requiring FVCOM outputs to be interpolated to a rectangular grid at each time step of the simulation, with implications for model accuracy and efficiency.

Simulating the fate and transport of microplastics in water is complex, owing in part to the fundamental complexities associated with driving physical processes in different aquatic environments. Zhang (2017) and Onink et al. (2019) describe the processes contributing to the transport of microplastic particles in coastal waters and oceans, respectively. The fate and transport of microplastics in water is also influenced by the physical properties of particles, particularly their density, size and shape (Khatmullina and Chubarenko, 2019). These properties may change over time in response to degradation (mechanical/chemical), growth of biofilm (Chubarenko et al., 2016; Rummel et al., 2017), coagulation (Long et al., 2015; Nizzetto et al., 2016), or fragmentation (ter Halle et al., 2016; Kaandorp et al., 2020) processes. The influence of these and other processes on the behaviour of plastic debris in the aquatic environment has been investigated in number of previous studies (Barnes et al., 2009; Quik et al., 2014; Chubarenko et al., 2016; ter Halle et al., 2016; Kaiser et al., 2017; Kooi et al., 2017; Michels et al., 2018; Hoellein et al., 2019; Li et al., 2019; Waldschläger and Schüttrumpf, 2019). Once microplastics are introduced into a water body, they move and disperse within the system in response to circulation patterns and diffusion processes. However, a certain fraction of the total microplastic particle load to the system may be trapped temporarily or permanently in stagnant regions (Monsen et al., 2002). The longer microplastic (polymer) particles are retained in a system, the more likely they are to be impacted by transformation processes such as weathering and degradation, release toxic ingredients (leaching), or absorb other ambient contaminants on their surface (Chamas et al., 2020; Zhang et al., 2021).

Recent advances in modeling the fate and transport of microplastics have mainly focused on implementing physical processes such as transport by Ekman and geostrophic currents (Onink et al., 2019), Stokes drift (Iwasakia et al., 2017), beaching and sedimentation (Liubartsevaa et al., 2018), buoyancy (Daily et al., 2020), and investigating the relative importance of various processes through sensitivity analyses. However, the performance of these models in simulating advection and dispersion of microplastic particles has never been thoroughly verified, which could be partly attributable to the lack of available measurements (laboratory or field). Previous modeling studies focussed on microplastics fate and transport have given limited attention to selecting appropriate numerical methods, which influence both computational efficiency and accuracy (e.g. Iwasakia et al., 2017; Alosairi et al., 2020; Daily et al., 2020). Optimizing computational efficiency and accuracy is particularly important for microplastics modeling, which require long simulations to characterize residence times, and capture gradual transformation processes over long time scales (e.g. degradation, biofouling). Compromising accuracy for computational efficiency can lead to accumulation of errors over time and degrade the utility of models as investigative and decision-support tools.

In this paper, the Canadian microplastic simulation (CaMPSim) system is presented as a novel and efficient numerical framework for predicting fate and transport of microplastics in rivers, lakes, estuaries, coastal waters and oceans, and is verified. The tool is based on a three-dimensional (3D) PTM model coupled with the TELEMAC hydrodynamic modeling system (Hervouet, 2007; Moulinec et al., 2011). The PTM incorporates innovative features that offer several advantages over existing models with respect to computational methodology and

modeling transport in aquatic environments with complex hydrodynamics. The Eulerian-Lagrangian model is based on an unstructured Eulerian mesh, considers both spatially and temporally varying diffusivity in the Lagrangian particle-tracking scheme, and uses an innovative method for locating particles ("point location") within the unstructured mesh. To the best of the authors' knowledge, these features have not previously been incorporated in PTMs for simulating fate and transport of microplastics. Verification of the PTM involved testing the accuracy of different advection schemes by comparing model predictions to known analytical solutions for idealized test cases. The potential real-world implications of selecting advection schemes with varying levels of accuracy and computational efficiency were explored using a previously calibrated and validated TELEMAC, three-dimensional hydrodynamic model of the lower Saint John River estuary in eastern Canada (Vouk et al., 2019).

2. Methodology

This section describes the methodology employed in CaMPSim-3D for modeling fate and transport of microplastics in water. The movement of microplastic particles in water is driven primarily by dynamic fluid and buoyancy forces due to ambient environmental conditions, and the physical characteristics (e.g., shape, size, density) of the particles. The physical characteristics of microplastics change over time in response to a variety of processes (transformation) that are, in turn, affected by ambient environment parameters (e.g., salinity, temperature, algae concentration, UV index). CaMPSim-3D has two main components: a Lagrangian component (i.e., PTM), which simulates particle advection, dispersion, buoyancy effect, transformation processes (biofouling, degradation), beaching and washing off, and an Eulerian component that provides the required information on ambient environment conditions for input to the PTM (e.g. water levels, velocities, turbulent viscosity, salinity, temperature, water density). The Eulerian model provides information on an unstructured (triangular) mesh. The Eulerian model may consist of multiple sub-models that compute hydrodynamics, waves, sediment transport, atmospheric conditions, depending on the complexity of the intended modeling and information needed for input to the PTM (Fig. 1). However, for the purpose of this study, which is focused on the numerical methodology of the PTM, the Eulerian model consists of a hydrodynamic model only.

2.1. Hydrodynamic model

The (Eulerian) hydrodynamic model is based on TELEMAC-3D, a three-dimensional, finite-element based, shallow water equations solver (Hervouet, 2007). The 3D computational mesh consists of triangular prism elements, generated by layering a series of plane, unstructured (triangular) meshes between the water surface and the bed. At each time step, the hydrodynamic model output is provided at the six vertices (x_i, y_i, z_i) of each triangular prism element within the computational domain (Fig. 2).

For the vertical discretization, either a sigma (bathymetrically conforming) or a fixed layer system can be adopted. If a sigma-layer system is chosen, the vertical position of vertices (z_i) will also be calculated at each time step of simulation. TELEMAC-3D provides multiple options for horizontal and vertical turbulence closure models, which can be used to calculate turbulent viscosity throughout the domain during the simulation. Assuming eddy viscosity (v) is equal to diffusivity (k) allows for spatially and temporally varying diffusivity to be estimated based on the eddy viscosity (v_{tx}, v_{ty}, v_{tz}) from output of the hydrodynamic model, and used as input to the PTM.

The TELEMAC-3D model is part of the TELEMAC modeling system, which comprises several additional modules that can be used to simulate wind waves, sediment transport and water quality. Here, the PTM relied only on information provided by the hydrodynamics module. The hydrodynamic model and the PTM were coupled 'offline', meaning that
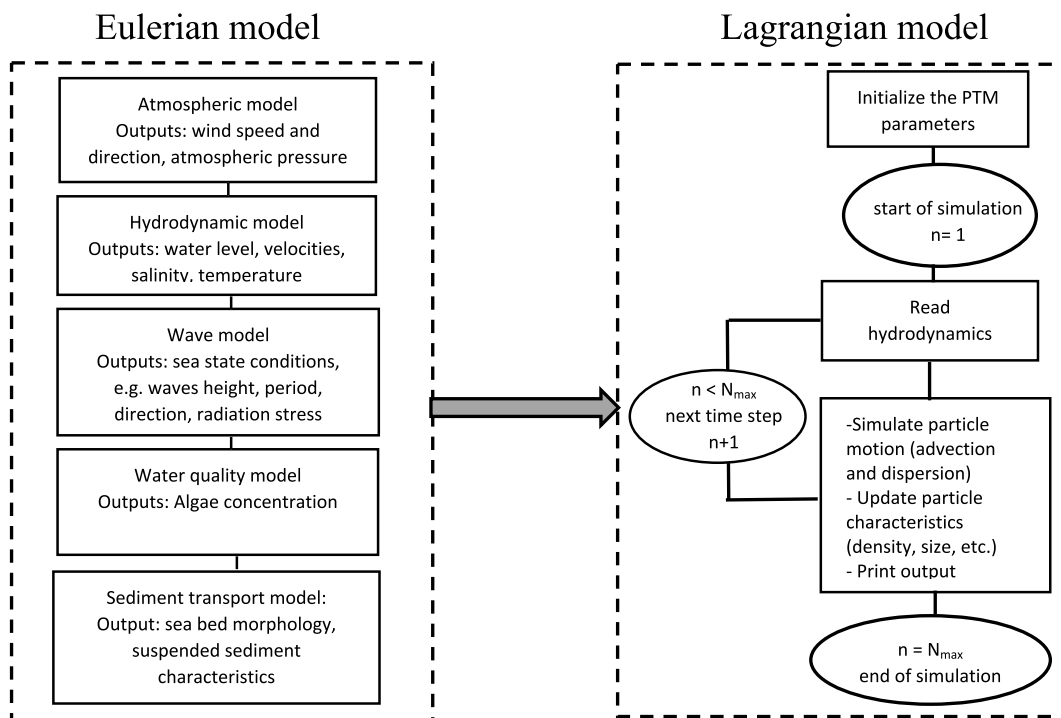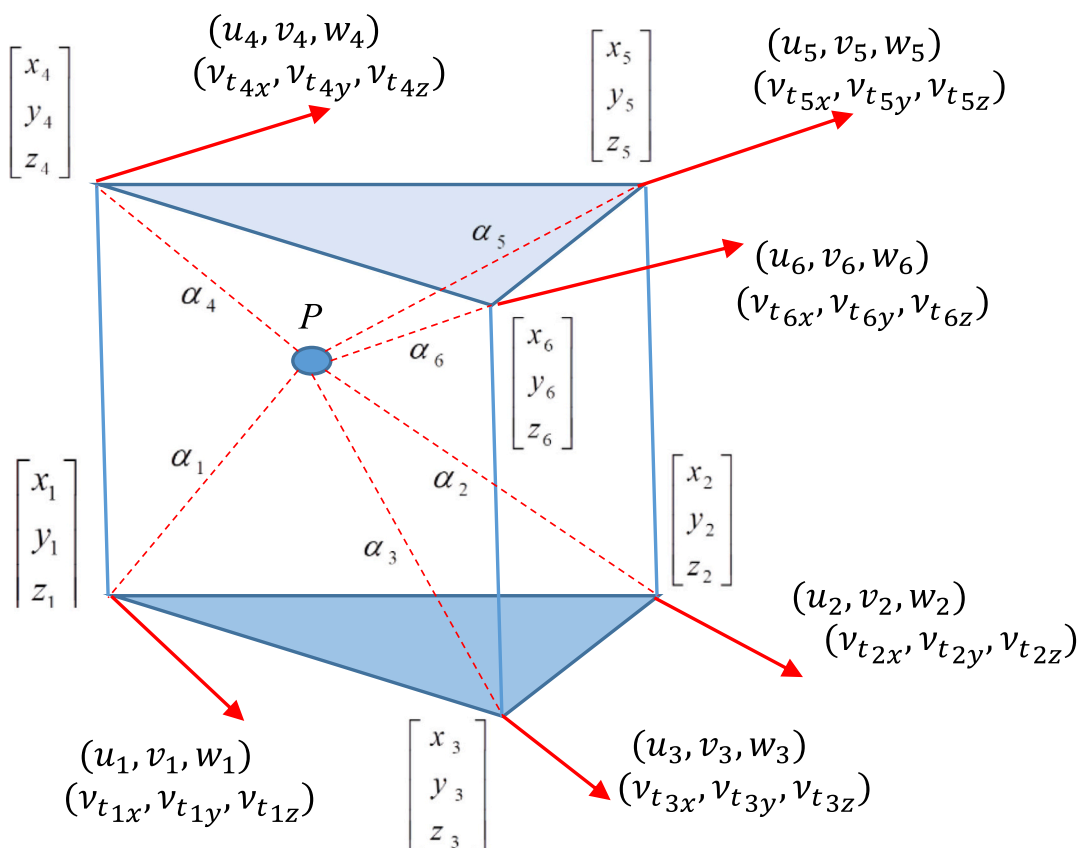
Eulerian model

Atmospheric model
Outputs: wind speed and
direction, atmospheric pressure

Hydrodynamic model
Outputs: water level, velocities,
salinity, temperature

Wave model
Outputs: sea state conditions,
e.g. waves height, period,
direction, radiation stress

Water quality model
Outputs: Algae concentration

Sediment transport model:
Output: sea bed morphology,
suspended sediment
characteristics

Lagrangian model

Initialize the PTM
parameters

start of simulation
n= 1

Read
hydrodynamics

$n < N_{max}$
next time step
n+1

-Simulate particle
motion (advection
and dispersion)
- Update particle
characteristics
(density, size, etc.)
- Print output

$n = N_{max}$
end of simulation

Fig. 1. CaMPSim-3D framework.

Fig. 2. A typical triangular prism cell in the TELEMAC-3D output. Water properties at the particle location are linked to 6 surrounding vertices based on the relative distances (αi).

information on hydrodynamics was passed to the PTM only, with no feedback.

2.2. Particle Tracking Model (PTM)

The three-dimensional PTM reads the computed velocity field (u_i, v_i, w_i), vertical elevations (z_i), and eddy viscosity (v_{tx}, v_{ty}, v_{tz}) from the output file of the TELEMAC-3D hydrodynamic model at each time step, and uses this information as the basis for computing the fate and transport of microplastics particles within the computational domain.

The PTM computations involve four main processes/steps, which are implemented for all particles at each time step of a simulation:

1) *Point location*, i.e., identification of the Eulerian mesh element in which the particle resides;
2) *Interpolation (spatially)* of hydrodynamic information from the Eulerian (hydrodynamic model) mesh to the particle position;
3) *Advection and dispersion*, i.e., simulation of particle transport;
4) *Transformation,* i.e., computing state variables and processes (e.g. biofouling, degradation).

The methodology for each of these processes is described below.

2.3. Point location

Finding the address of the Eulerian mesh element containing a particle (host element) is a computationally demanding (i.e., time-consuming) process for PTMs that are coupled with Eulerian models utilizing unstructured grids. The process is generally known as the "point location" problem (de Berg et al., 2008) in the computational geometry context. Examples of different methodologies aimed at optimizing point location queries in planar (2D) and spatial (3D) spaces are described by Kirkpatrick (1984) and Preparata and Tamassia (1992). By contrast to unstructured meshes, point location within uniform, regular Cartesian grids is straightforward. To take advantage of efficiencies, a Cartesian-based method is therefore used here to locate points within the unstructured Eulerian mesh. A Cartesian grid is generated, overlaying the Eulerian model unstructured mesh (Fig. 3). Each rectangular cell of the Cartesian grid is called a Zone (dashed line in Fig. 3). The triangular mesh elements occupying each Zone are identified only once at the beginning of the simulation, which makes the approach computationally efficient. At each time step of the simulation, the Zone in which each particle is located is first identified. Only triangular elements located within the Zone associated with each particle are then searched to assign elements to their respective particles.

2.4. Interpolation

Prior to computing advection and dispersion of particles, the PTM requires that input from the Eulerian (hydrodynamic) model be trans-
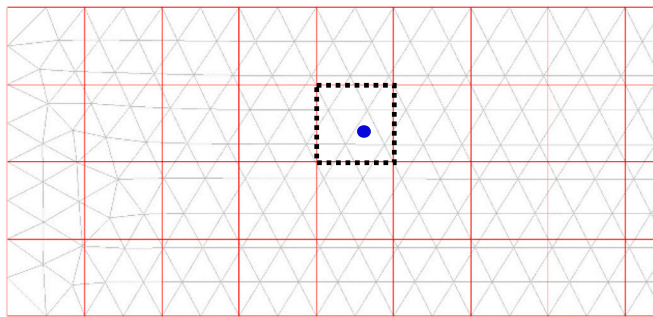

Fig. 3. Schematic of point location method. Black dashed line represents a Zone on the background Cartesian grid.

formed to the Lagrangian frame of reference, by mapping or interpolating hydrodynamic parameters in space to each particle. However, the choice of interpolation method can significantly affect accuracy and computational efficiency. A comparison of some interpolation methods is provided in Jacob et al. (2007) and van Hinsberg et al. (2013). Here, a computationally efficient inverse distance weighted (IWD) scheme (Chen et al., 2015) was employed, whereby the value of any parameter B_p at X_p (the position of particle P) is calculated based on the discrete values of the parameter (B_i) at the six vertices of the encompassing element ($i = 1$ to 6) and the distances between the particle and each of the vertices (α_i in Fig. 2), i.e.:

$$B_p = \sum_{i=1}^{6} \frac{1}{\alpha_i} B_i \Big/ \sum_{i=1}^{6} \frac{1}{\alpha_i} \tag{2}$$

2.5. Advection and dispersion

Following conventional particle-tracking model formulations, the change in position of a particle in response to advection and diffusion over a discrete time step (Δt) can be described by (Lebreton et al., 2012; Kako et al., 2011; Yoon et al., 2010; Jalón-Rojas et al., 2019):

$$\frac{dx_p}{dt} = Adv + Diff \tag{3}$$

where $x_p(t)$ represents the position (in three-dimensional Euclidean space) of particle P at time t. The advection term (Adv) in Eq. (3) represents transport of the particles by the ambient velocity field. The above equation belongs to the general family of Langevin equations (Nandakumar, 2021).

Using a kinematic approach, PTM models normally use $Adv = U_p$ where U_p is the particle velocity calculated from Eq. (2) (Jalón-Rojas et al., 2019; Liubartseva et al., 2018).. In addition to advection and diffusion, the displacement in time of particles in the vertical direction is influenced by their settling/rising velocities. The vertical component of the particles velocity (w_p) is calculated based on Eq. (4) where w_s, depending on the relative density to water (RD), may be negative for settling particles (for $RD > 1$), or positive for buoyant particles ($RD < 1$). The settling/rising velocity of a particle is linked to its physical properties (i.e. dimension, shape, gravity), and is normally calculated from empirical relationship derived from laboratory testing. The settling/rising velocity of a particle is linked to its physical properties (i.e. dimension, shape, gravity), and is normally calculated from empirical relationship derived from laboratory testing.

$$w_p = \frac{\sum_{i=1}^{6} \frac{1}{\alpha_i} w_i}{\sum_{i=1}^{6} \frac{1}{\alpha_i}} + w_s \tag{4}$$

In CaMPSim, w_s is calculated from Eq. 5 based on the Newton's impact formula (Dellino et al., 2005) where d_* is the diameter of an equivalent sphere, ρ is the water density, ρ_p is the particle density, g is the gravity acceleration, and C_D is the drag coefficient calculated using Eq. 6 (Dioguardi et al., 2017) as a function of particle shape factor ψ and particle Reynolds number (Re_p). Eq. 6 is applicable to all main shape classes of microplastics (i.e. spheres, fragments, fibres and films), and has been identified by Van Melkebeke et al. (2020) as the most appropriate drag model for describing sinking behaviour of microplastics.

$$w_s = \sqrt{\frac{4}{3} \frac{d_*}{C_D} \left| \frac{\rho_s - \rho}{\rho} \right| g} \tag{5}$$

$$C_D = \frac{24}{Re_p} \left(\frac{1-\psi}{Re_p} + 1 \right)^{0.25} + \frac{24}{Re_p} \left(0.1806 Re_p^{0.6459} \right) \psi^{-Re_p^{0.08}} + \frac{0.4251}{1 + \frac{6880.95}{Re_p} \psi^{5.05}} \tag{6}$$

In the test cases investigated in this study, all particles were assumed to be neutrally buoyant and mass-/dimension-less, such that eqs. 5 and 6 were not activated in the model. A first-order approximation of the advection term is $Adv = U_p$. For a more accurate treatment of advection, a second-order approximation of the advection term was applied following Iwasakia et al. (2017):

$$Adv = U_p + \frac{DU_p}{Dt} U_p \Delta t \tag{7}$$

where

$$\frac{DU_p}{Dt} = \frac{1}{2} \left(U \bullet \nabla U + \frac{\partial U_p}{\partial t} \right) \tag{8}$$

where U_i (u_i, v_i, w_i) is the three-dimensional velocity vector provided by the hydrodynamic model on the Eulerian grid. In Eq. 8, the velocity gradient in the horizontal direction is calculated by averaging the gradient values for the top and bottom (triangular) faces of the cell, following the approach of (Mohammadian and Le Roux, 2006), i.e.:

$$\left(\frac{\partial U}{\partial x} \right) = \frac{1}{A_i} \int \frac{\partial U}{\partial x} dA \approx \frac{C_1 \Delta y_1 + C_2 \Delta y_2 + C_3 \Delta y_3}{A_i} \tag{9}$$

$$\left(\frac{\partial U}{\partial y} \right) = \frac{1}{A_i} \int \frac{\partial U}{\partial y} dA \approx \frac{C_1 \Delta x_1 + C_2 \Delta x_2 + C_3 \Delta x_3}{A_i} \tag{10}$$

$$A_i = \frac{1}{2} [(x_2 y_3 - x_3 y_2) - (x_1 y_3 - x_3 y_1) + (x_1 y_2 - x_2 y_1)] \tag{11}$$

where A_i is the area of the top and bottom triangular face of the cell (Fig. 2). Other parameters in Eqs. 9 and 10 are defined as,

$$\Delta x_1 = x_3 - x_2 \qquad \Delta y_1 = y_3 - y_2 \tag{12}$$

$$\Delta x_2 = x_1 - x_3 \qquad \Delta y_2 = y_1 - y_3 \tag{13}$$

$$\Delta x_3 = x_2 - x_1 \qquad \Delta y_3 = y_2 - y_1 \tag{14}$$

$$C_1 = \frac{1}{4} (U_2 + U_3 + U_5 + U_6) \tag{15}$$

$$C_2 = \frac{1}{4} (U_1 + U_3 + U_4 + U_6) \tag{16}$$

$$C_3 = \frac{1}{4} (U_1 + U_2 + U_4 + U_5) \tag{17}$$

The velocity gradients in the vertical direction $(\partial U/\partial z)$ are calculated for corresponding (overlaying) nodes on top and bottom (triangular) faces of the cell, and mapped/interpolated to each particle using the IWD method. The second term on the right-hand side of Eq. 3 (*Diff*) represents the effect of turbulent diffusion (and dispersion arising from velocity gradients not resolved by the computational mesh) on particle motion. Diffusion or dispersion of particles may be approximated as a random walk process, i.e., $Diff = \frac{R}{\Delta t} \sqrt{2K \Delta t}$, where R is a random number between -1 and 1 from a standard normal distribution, and K is the diffusion (or dispersion) coefficient (Israelsson et al., 2006; Salamon et al., 2006). This formulation is referred to as the naïve random walk model (Hunter et al., 1993; Visser, 1997), and is based on the assumption that K is uniform in space and constant in time. However, this assumption is violated in many aquatic environments where turbulence properties vary in time and space. Under such conditions, the naïve random walk model can lead to artificial accumulation of particles in high actual diffusivity regions (Hunter et al., 1993; Visser, 1997). Here, as novel approach in the context of microplastics fate and transport modeling, a modified diffusion term (Hunter et al., 1993) is employed to correct for such errors, i.e.:

$$Diff = \frac{\partial K_p}{\partial X} + \frac{R}{\Delta t} \left\{ \sqrt{2K_p \left[X_p(t) + \frac{1}{2} \frac{\partial K_p}{\partial X} \Delta t \right] \Delta t} \right\} \tag{18}$$

where K_p represents the diffusivity coefficient at X_p at time t, and is calculated based on Eq. (2) using the eddy viscosities (ν_t) provided by the hydrodynamic model on the Eulerian grid, and assuming the turbulent Schmidt number, $Sc_t = \nu_t / K_p = 1$. If the diffusivity coefficient is uniform in space, $\partial K_p/\partial X = 0$ in Eq. 18 and the diffusive random walk model simplifies to the naïve random walk model.

The particles that collide horizontally (land/shoreline) or vertically (bed/water surface) with the model boundaries will continue to move along the boundary without any influence from the wall, which is also known as a free-slip boundary condition. However, CaMPSim includes a provision for parameterizing particle interaction with the bed (deposition and re-suspension) and land (beaching and washing off). However, these processes were not activated in this study. Sedimentary processes are expected to be governed, in part, by bottom shear stress, which can be provided by the hydrodynamic model. Thresholds for deposition or incipient motion of plastic particles depend on parameters such as particle size, geometry, and density. Parameterization of these processes will rely heavily on previous applications of particle-tracking models for sediment transport problems (e.g. Herrera-Díaz et al., 2017; Barati et al., 2018) while taking into account aspects specific to microplastics (Liubartseva et al., 2018; Jalón-Rojas et al., 2019) such as the effects of biofouling on polarity and adhesiveness (Wu et al., 2020; Van Melkebeke et al., 2020).

2.6. Transformation

Changes in the physical properties of microplastics (transformation) in a water environment can be caused by a variety of processes such as aggregation with other suspended particles or sediments, the formation of biofilms (biofouling) on the surface of particles, and fragmentation to smaller particle sizes caused by degradation processes (Weinstein et al., 2016; Jahnke et al., 2017; Kaandorp et al., 2021). All transformation processes are generally influenced by two groups of parameters: 1) the ambient environmental conditions such as water temperature, salinity, pH and ultraviolet light exposure, and 2) the physio-chemical characteristics of the particles such as polymer type, size, shape, and density. The transformation processes influence the transport of microplastic particles in water by modifying the particle properties, and consequently, the hydrodynamic forces.

CaMPSim can simulate, using empirically derived relationships to ambient water conditions, particle size changes resulting from transformation processes including biofouling (Kooi et al., 2017), and degradation (Jalón-Rojas et al., 2019).

3. Numerical solution

This section describes the numerical methodology employed in the PTM for solving the advection-diffusion equation (Eq. 2). The numerical schemes employed in the model for solving advection and diffusion processes are discussed separately in this section. For each process, the model performance is assessed by comparing the results of simulations with known analytical solutions for test cases.

3.1. Advection

The importance of using an accurate numerical scheme for advection in PTMs has been discussed by Wolk (2003), Lee et al. (2013) and Gräwe et al. (2012). Complex, high-order numerical methods generally provide more accurate predictions than simple, low-order methods. However, higher-order schemes are generally associated with a higher computational cost. Balancing accuracy requirements with computational efficiency is a key consideration in choosing appropriate numerical

methodologies for PTMs, particularly for applications that consider transport and other processes that span long temporal and large (regional) spatial scales. For long simulations, small errors in computing particle velocities or translations can accumulate over time, and lead to significant errors in predicted pathways and the fate of particles. Here, six popular numerical advection schemes are investigated: Euler, Second-order Runge–Kutta (RK2), Third-order Runge–Kutta (RK3), Fourth-order Runge–Kutta (RK4), Second-order Total Variation Diminishing (TVD2) Runge-Kutta, Third-order Total Variation Diminishing (TVD3) Runge–Kutta, and Second-order Adams-Bashforth (AB). Formulations of these methods are summarised in Table 2, where superscripts n and $n + 1$, denote variables at time t and $t + \Delta t$, respectively.

The accuracy of each scheme was assessed by comparing the modeled results to known analytical solutions for four 2D and one 3D test cases (*analytical tests*). For each test case, a specific velocity field was generated on a uniform, unstructured mesh, consisting of triangular (2D) or triangular prism (3D) elements with characteristic edge lengths equal to 10 cm. One particle was released in the computational domain and the trajectory computed by the numerical model was compared with the analytical solution. A summary of the analytical tests specifications including information on the velocity field and the particle trajectory is provided in Table 3. The time step was 0.1 s in all tested cases. The performance of numerical methodology was analyzed through calculating the Root Mean Square Error *(RMSE)*, and normalized Mean Absolute Error (*NMAE*):

$$RMSE = \sqrt{\frac{1}{M} \sum_{m=1}^{M} \sum_{j=1}^{3} \left(X_{p_{Modeled}} - X_{p_{Analytic}} \right)^2} \qquad (19)$$

$$NMAE = \frac{1}{M} \sum_{m=1}^{M} \frac{1}{3} \sum_{j=1}^{3} \left| \frac{X_{p_{Modeled}} - X_{p_{Analytic}}}{X_{p_{Analytic}}} \right| \qquad (20)$$

where M is the total number of modeled particles, $X_{p_{Modeled}}$ and $X_{p_{Analytic}}$ are vectors representing the particle position in 3D space (x,y,z) based on the model results and the analytical solution respectively.

Table 2
Formulations of the examined numerical schemes for the advection process.

Order	Method	Formulation
First-order	Euler	$X^{n+1} = X^n + U(x_p^n, y_p^n)\Delta t$
Second-order	Adams-Bashforth (AB)	$X^{n+1} = X^n + \frac{3}{2}U\left(x_p^n, y_p^n\right)\Delta t - \frac{1}{2}U\left(x_p^{n-1}, y_p^{n-1}\right)\Delta t$
	Runge–Kutta (RK2)	$X^{n+1} = X^n + U\left(x_p^{n+\frac{1}{2}}, x_p^{n+\frac{1}{2}}\right)\Delta t$
	Runge-Kutta (TVD2)	$X_*^{n+1} = X^n + U(x_p^n, y_p^n)\Delta t$ $X^{n+2} = X_*^{n+1} + U(x_p^{*n+1}, y_p^{*n+1})\Delta t$ $X^{n+1} = \frac{1}{2}\left(X^n + X^{n+2}\right)$
Third-order	Third-order Total Variation Diminishing Runge–Kutta (TVD3)	$X^* = X^n + U(x_p^n, y_p^n, t^n)\Delta t$ $X^{**} = \frac{3}{4}X^n + \frac{1}{4}X^* + \frac{1}{4}U\left(x_p^*, y_p^*, t^{n+1}\right)\Delta t$ $X^{n+1} = \frac{1}{3}X^n + \frac{2}{3}X^{**} + \frac{2}{3}U\left(x_p^{**}, y_p^{**}, t^{n+1/2}\right)\Delta t$
Fourth-order	Runge–Kutta (RK4)	$X^{n+1} = X^n + \frac{1}{6}(k_1 + 2k_2 + 2k_3 + k_4)\Delta t$ $k_1 = U(x_p^n, y_p^n)$ $k_2 = U\left(x_p^{n+\frac{1}{2}} + k_1\frac{\Delta t}{2}, y_p^{n+\frac{1}{2}} + k_1\frac{\Delta t}{2}\right)$ $k_3 = U\left(x_p^{n+\frac{1}{2}} + k_2\frac{\Delta t}{2}, y_p^{n+\frac{1}{2}} + k_2\frac{\Delta t}{2}\right)$ $k_4 = U(x_p^{n+1} + k_3\Delta t, y_p^{n+1} + k_3\Delta t)$

3.2. Diffusion

The PTM performance in simulating diffusion was evaluated by comparing the model results to the analytical solution of the diffusion equation (Eq. 21) for a one-dimensional test case. The initial condition was an instantaneous release of 250,000 particles, following a Gaussian distribution. Following the release, the particles were allowed to move in response to diffusion only (Eq. 2). Over 100 s were simulated with time step of 0.1 s using naïve random walk formulation with constant diffusion coefficient $K = 0.001$ m²/s.

$$C(X, t) = \frac{C_0}{\sqrt{4\pi K}} e^{\frac{-(X)^2}{4Kt}} \qquad (21)$$

To convert PTM output (particle positions) to concentrations for comparison to the analytical solution of the diffusion equation, a rectangular structured grid with a uniform cell size of 5 cm was created. This cell size was chosen based on a sensitivity analysis to ensure the effect of grid resolution on the model results is <3 %. For each cell, the concentration at any time was computed as the ratio of the number of particles occupying the cell to the total number of particles released in the model.

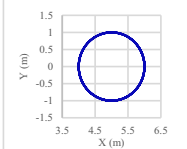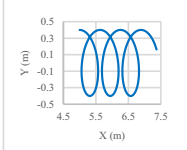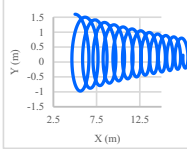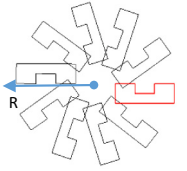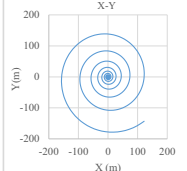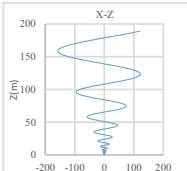### 3.3. Sensitivity test to advection schemes

The influence of the Advection scheme methodology on PTM analysis for a real-world application (lower Saint John River estuary, in eastern Canada) was investigated. The PTM was used to simulate advection and dispersion of particles representing microplastics in an approximately 75-km long reach of the Saint John River from Evandale to the Bay of Fundy (Fig. 4). The PTM model used the velocity field, water levels, and eddy viscosity field from a TELEMAC-3D hydrodynamic model previously developed by Vouk et al. (2019) to simulate dispersion and transport of effluent plumes within the Saint John River estuary. The hydrodynamic model is driven by fluvial flows at two upstream boundaries and tidal elevations at the downstream boundary in the Bay of Fundy. The hydrodynamic model was previously calibrated and validated previously using water levels, velocities, and salinity and temperature profiles at several locations. Multiple scenarios were simulated using the various numerical schemes (Euler, RK2, RK3, RK4, TVD2, TVD3, AB), and the influence of numerical methods in predicting particles accumulation zones was analyzed.

The particles were assumed neutrally buoyant and massless. Two scenarios were simulated, referred to as Sc1 and Sc2. In Sc1, 62,868 particles were initially distributed uniformly throughout the computational domain at horizontal intervals of 75 m (in both north-south and east-west directions). The duration of the Sc1 simulation was 15 days, spanning one full spring-neap tidal cycle. For Sc2, 6811 particles were uniformly distributed at 25 m horizontal intervals within Zone 1 (Fig. 4), and their movement was simulated for 7 days. Both Sc1 and Sc2 simulations were conducted following an initial 11-day spin-up period of the hydrodynamic model. The PTM time step was 15 min, which was set based on the time step of the output from the hydrodynamic model.

4. Results and discussion

The boxplot graphs in Fig. 5 represent comparison of RMSE and NMEA for the examined advection schemes in the analytical tests (Table 3). For each box, the upper and lower whiskers show the maximum and minimum, respectively, and the horizontal bar in the center of the box represents the median. RK4 showed the best performance (i.e. the minimum average RMSE and NMAE) among the employed advection schemes, followed by TVD3 and RK2, respectively. Despite having the same order of accuracy, the RK2 method generally showed a better performance than TVD2 in all of the analytical test cases. As expected, the Euler method, which is the lowest order method examined here, performed worst in terms of particle advection accuracy.

Table 3

Specification of the analytical test cases used to evaluate the advection schemes.

Test number	Velocity field	Particle trajectory	Particle trajectory shape
Test1 (Fabbroni, 2009)	$u = u_0 \cos(\omega t)$ $v = -v_0 \sin(\omega t)$ $u_0 = 0.5$ $\omega = 1.0$	$x = x_0 + \dfrac{u_0}{\omega} \sin(\omega t)$ $y = y_0 - \dfrac{u_0}{\omega}(1 - \cos(\omega t))$	
Test2 (Fabbroni, 2009)	$u = u_g + u_0 \cos(\omega t)$ $v = -(u_0 - u_g)\sin(\omega t)$ $u_0 = 0.5$ $u_g = 0.1$ $\omega = 1.0$	$x = x_0 + u_g t + \dfrac{u_0 - u_g}{\omega} \sin(\omega t)$ $y = y_0 - \dfrac{u_0 - u_g}{\omega}(1 - \cos(\omega t))$	
Test3 (Fabbroni, 2009)	$u = u_g e^{-\gamma t} + (u_0 - u_g)e^{-\gamma t} \cos(\omega t)$ $v = -(u_0 - u_g)e^{-\gamma t} \sin(\omega t)$ $u_0 = 1.2$ $u_0 = 0.15$ $\gamma = 0.01$ $\gamma_g = 0.01$	$x = x_0 + \dfrac{u_g}{\gamma_g}(1 - e^{-\gamma t})$ $+ \dfrac{(u_0 - u_g)\omega}{\omega^2 + \gamma^2}$ $\left[\dfrac{\gamma}{\omega} + e^{-\gamma t}\left(\sin(\omega) - \dfrac{\gamma}{\omega}\cos(\omega)\right)\right]$ $y = y_0 - \dfrac{(u_0 - u_g)\omega}{\omega^2 + \gamma^2}$ $\left[1 - e^{-\gamma t}\left(\cos(\omega) + \dfrac{\gamma}{\omega}\cos(\omega)\right)\right]$	
Test4	$u = \omega y$ $v = -\omega x$ $\omega = 0.0628$	$x^2 + y^2 = R/_{2\pi}$	
Test5 (Strang, 2016)	$u = \alpha\beta \exp(\beta t)\cos(\gamma t) - \gamma \exp(\beta t)\sin(\gamma t)$ $v = \alpha\beta \exp(\beta t)\sin(\gamma t) + \gamma \exp(\beta t)\cos(\gamma t)$ $w = \alpha\beta \exp(\beta t)$ $\alpha = 0.8$ $\beta = 0.12$ $\gamma = 1.5$	$x = \alpha \exp(\beta t)\cos(\gamma t)$ $y = \alpha \exp(\beta t)\sin(\gamma t)$ $z = \alpha \exp(\beta t)$	

In most of the analytical test cases, the calculated error for the Euler method is orders of magnitude higher than other methods, illustrating the importance of using higher order schemes in Lagrangian simulations. For example, an error associated with the Euler scheme for a particle transported in analytical test case 3 can cause >1.5 km deviation in the particle position over a period of 10 days compared to <1 cm deviation with RK4 scheme. The AB advection scheme gave the highest errors among the higher order methods investigated.

In order to analyse the temporal accuracy of the model, a systematic error analysis was performed by successively reducing time step sizes and monitoring the local error, which is defined as:

$$Err_{Local} = X_{Analytic} - X_{Numeric}$$

at time $t = 10$ s for Test 1 (described in Table 3). Fig. 6 illustrates the error generated by different advection schemes examined in this study. As shown in Fig. 6, the convergence of plotted errors corresponded to a theoretical order of accuracy in the log-log coordinate equal to 1, 2 and 4 for the first-order (Euler), second-order (RK2, TVD2) and fourth-order (RK4) schemes, respectively. The slope of the line drawn through plotted local errors for the TVD3 was similar to the RK4 scheme, which

indicates that the accuracy of TVD3 exceeded the theoretical accuracy of a third order-scheme.

For the diffusion test case, the analytical solution were compared to the numerical model (PTM) results at different snapshots of a 100 s simulation in Fig. 7. The advection process was not simulated in this test. The correlation between the numerical model predictions and the analytical solution for the diffusion test case is shown in Fig. 8, with a correlation coefficient of $R^2 = 0.9966$.

All simulations conducted for Sc1 indicated that Zone 1 and Zone 2 (Fig. 4) represented trap areas for particles introduced to the Saint John River system. The influence of using different advection scheme on the PTM predictions was assessed by comparing the ratio of number of particles residing in Zone 1 (N_{p1}) and Zone 2 (N_{p2}) to the total number of particles (N_{ptotal}) over the simulation period (Fig. 9). Sc1 resulted in an increasing number of particles in Zones 1 and 2 over the simulation period, for all 6 advection schemes tested. RK4 (the most accurate scheme based on the analytical tests) predicted the slowest rate of particle accumulation in Zone 1 and the highest rate of accumulation in Zone 2. The TVD3 method provided the closest results to RK4 in terms of predicting the number of particles in each zone (Fig. 9). The TVD2 and
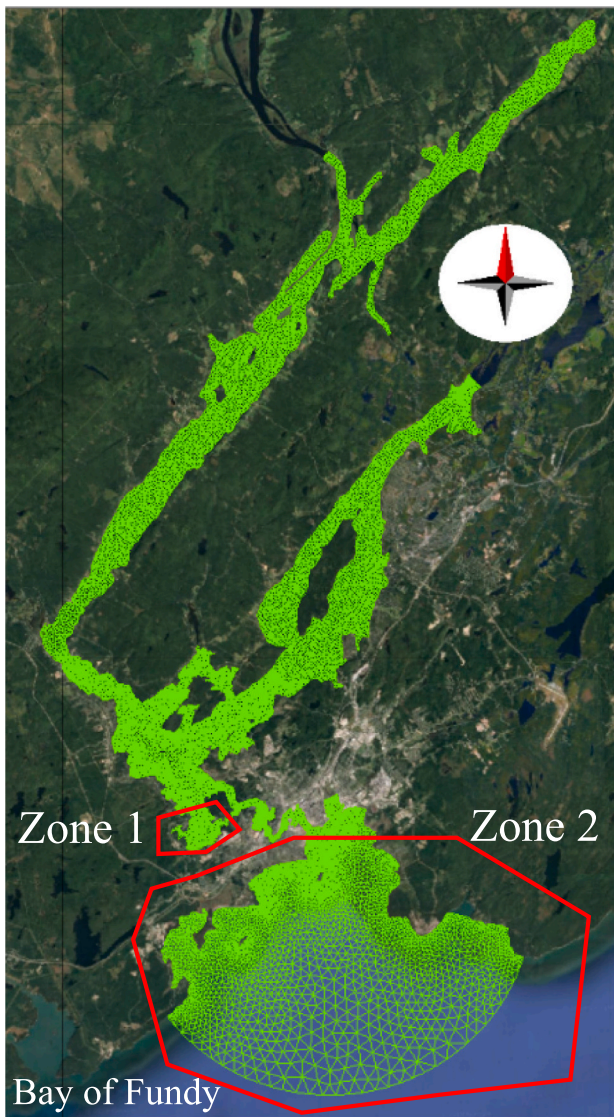
Fig. 4. Computational grid of the hydrodynamic model.

TVD3 methods showed similar performance in predicting the number of particles in Zone 1 and Zone 2 for Sc1.

In addition to accuracy, computational cost is another important factor influencing selection of methodology for a numerical model. An optimum numerical method provides a balance between accuracy and computational cost based on characteristics of the intended application. To illustrate the computational demand of the advection schemes in this study, the time required to simulate 500 time steps (125 h) of Sc1 with different advection schemes on a an Intel Core i7 workstation with 2.0 GHz CPU and 8 GB of RAM is compared in Fig. 10. The most accurate advection scheme (RK4) took twice as long as the AB and Euler methods to complete the simulation. The computational costs of the TVD2 and TVD3 schemes are approximately 21 % and 27 % faster than the RK4 method, respectively. The RK2 method, the third most accurate advection method was 31 % slower than the fastest methods (Euler and AB), and approximately 37 % faster than the RK4 method (the slowest but most accurate method).

Addition of the second term in the advection equation (Eq. 7) showed negligible influence on the model results in the analytic tests but caused approximately 67 % increase in the number of particles in Zone 1 after 4 days of the Sc1 simulation with RK4 advection scheme (Fig. 11). The extra computation imposed by addition of the second term also increase computational cost of the simulation by 15 %. The significant influence of the second term on the model results is attributable to strong spatial and temporal gradients of the ambient velocity field resulted from complex morphology and highly variable discharge of the Saint John River estuary.

The influence of employing a spatio-temporally varying diffusion coefficient (modified random walk model) on the PTM predictions was investigated for Sc1. The number of particles in Zone 1 after 480 steps (4 days) of simulation predicted by the modified random walk model with the RK4 advection scheme was compared to the number of particles predicted by the naïve random walk model (Fig. 12). The naïve random walk model was tested for 7 different configurations for combinations of 2 horizontal ($K_h = 1$, 10 m^2/s) and 4 vertical ($K_v = 10^{-5}$, 10^{-4}, 10^{-3}, 10^{-2} m^2/s) diffusivity coefficients. The configurations were selected based on the ranges of the horizontal and vertical eddy viscosities calculated by the hydrodynamic model. In general, the naïve random walk model predicted a more rapid accumulation in Zone 1 over the first 2 days of the simulations, seemingly consistent with arguments by Hunter et al. (1993) and Visser (1997) that the naïve random walk model may cause artificial accumulation of particles in low diffusivity regions. Lower horizontal diffusion coefficients predicted faster accumulation of particles in Zone 1 during the first 12 h of the simulations. By contrast to the modified random walk model, the naïve random walk model predicted a gradual decrease in the number of particles in Zone 1 from day 2 of the simulation, with more particles retained for higher vertical diffusion coefficients. This suggests that, despite initially predicting increases in the number of particles retained in low diffusivity
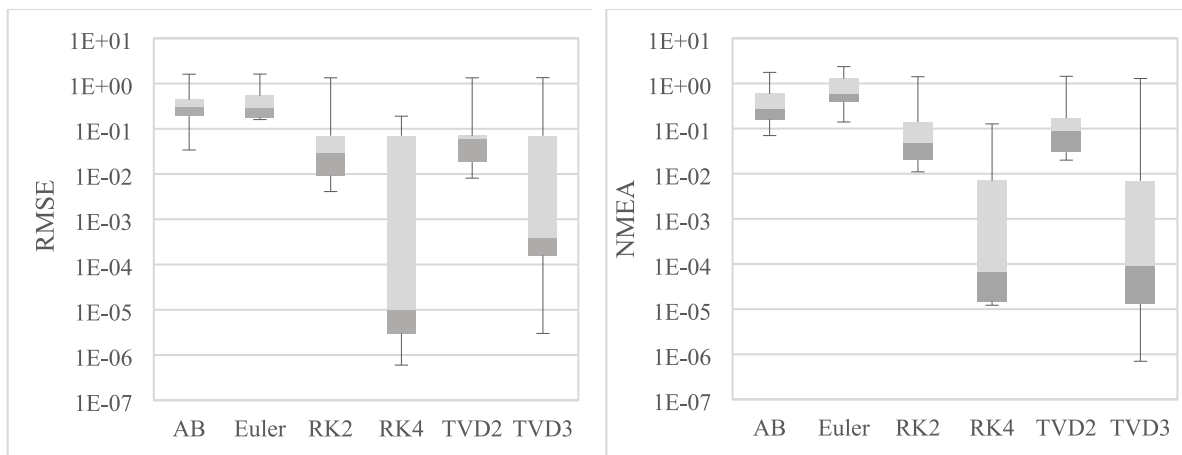

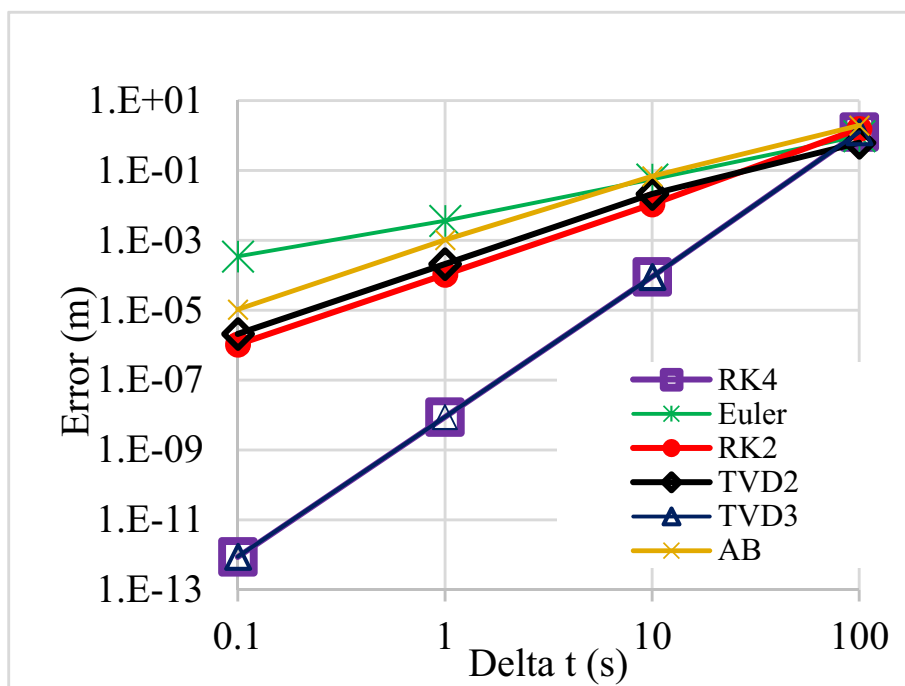**Fig. 5.** RMSE (Left) and NMEA (Right) across all analytical tests by advection scheme.

Fig. 6. Local error of the numerical solution of Test 1 (Table 3) at t = 10 s for the tested numerical schemes in this study in the log-log coordinate.
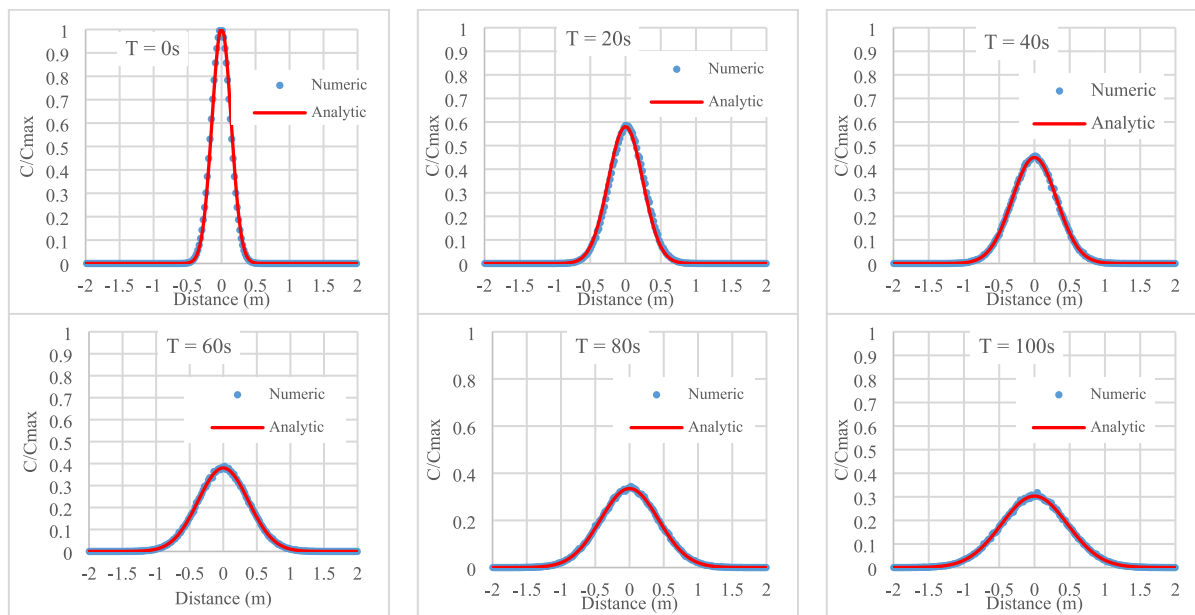

Fig. 7. Snapshots of the numerical model results and the analytical solution for diffusion test.

regions, application of the naïve random walk model in PTMs could ultimately underestimate residence times of particles in these regions.

For the Sc2 simulation, the particle count within Zone 1 over time is presented in Fig. 13. The results show that between 81 % and 98 % (depending on the advection scheme) of particles released into Zone 1 remained trapped in the region over the entire 15-day simulation period. The number of particles in Zone 1 at the end of the simulation was approximately 9 % higher using TVD2 than TVD3. The number of particles remaining in Zone 1 applying the RK2 and Euler methods was resulted in up to 3 times larger than the model predictions with the RK4 method. Approximately 5 to 10 % of the particles released into Zone 1 exit the region within the first five time steps of the simulation (Fig. 13). However, this sharp drop in the number of particles within Zone 1

recovers within the next 24–48 time steps (i.e. 6–12 h) as particles re-enter the zone, for all advection schemes except RK4 and TVD3. This behaviour is associated with strong temporal and spatial gradients in the ambient velocity field and complex system hydrodynamics, driven by strong and highly variable tides in the Bay of Fundy and fluvial flows.

Comparison of the Sc1 and Sc2 model results for different advection schemes reveals significant sensitivities to the advection scheme. Appropriate selection of advection schemes is therefore likely to be important in accurately and realistically predicting fate and transport of microplastics in real world settings.

In summary the model demonstrated to be able to successfully simulate transport of particles in a variety of test cases representing 2D and 3D conditions. Although in all of the test cases investigated in this
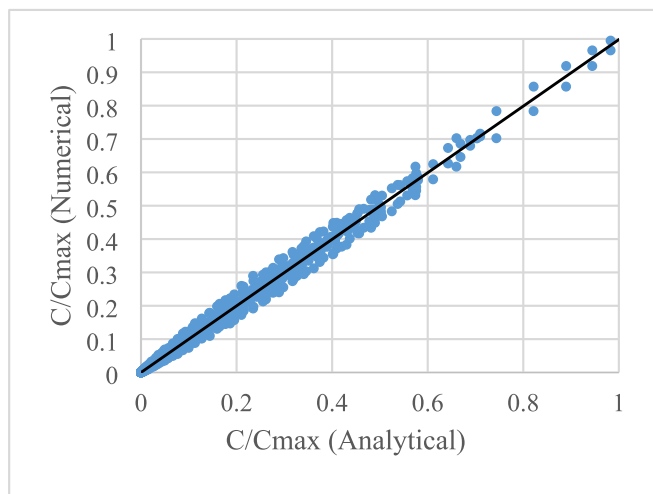
Fig. 8. Correlation between numerical predictions and analytical solution for the instantaneous Gauss-distributed particle release test case for diffusion.

study particles were assumed to be neutrally buoyant and mass-/dimension-less, the model has built-in capabilities to incorporate the influence of particles physical characteristics (i.e. shape, size, density) on the transport process. Biofouling and degradation processes can be simulated by the model. Coagulation process is not currently implemented in the model. Free-slip boundary conditions were applied in all of the tests. The diffusion validation test was conducted using constant diffusivity, whereas the Saint John River simulations were conducted using variable diffusivity feature of the model. The model has other potential capacities such as modeling beaching and washing-off processes, and considering the influence of wind and wave actions on particles transport which were not presented here.

5. Summary and conclusion

In this study a 3D numerical particle tracking model (PTM) was developed and coupled with TELEMAC-3D hydrodynamic model, to provide a new framework (CaMPSim-3D) for simulating transport of microplastics in rivers, lakes, estuaries, coastal waters, and oceans. The PTM calculates movement of microplastics in different water settings based on the information provided by the hydrodynamic model. The PTM works with a hydrodynamic model based on an unstructured grid. This unique feature, which is not available in most of the previous models, makes the PTM an appropriate choice for modeling

microplastics transport in aquatic environments with irregular geometries and complex hydrodynamics such as rivers and estuaries.

The study also investigated the influence of different advection schemes on the PTM accuracy and computational efficiency. Six numerical schemes with different levels of complexity were selected, and their performance with respect to the computational demand and predicted results were compared for a series of analytical tests, and a real world model of the lower Saint John River estuary. Significant differences were observed between the Euler method (traditionally used in PTMs) and higher order schemes, demonstrating the importance of using more accurate advection schemes in the PTM. The RK4 method provided the most accurate predictions in the analytical test. The TVD3 method provided results that were reasonably consistent with RK4 with approximately 27 % lower computational cost. For a quiescent bay on the periphery of the main channel of Saint John River estuary (Zone 1), the standard Euler advection scheme predicted approximately 13 % higher particle retention compared to the most accurate scheme (RK4). The observed sensitivity to the employed advection scheme demonstrates the importance of the numerical method in accurately predicting residence times in real-world settings, with knock-on implications for predicting time-dependent microplastic transformation processes, and ultimately, environmental effects.

The PTMs capability to incorporate spatio-temporally varying diffusivities (i.e., the modified random walk) is deemed an important improvement over existing PTMs used for modeling microplastic fate and transport, for reasons described by other authors (e.g. Hunter et al., 1993; Visser, 1997). Compared to the naïve random walk model, the modified random walk model predicted a two-fold difference in the number of particles accumulated in a side bay of the Saint John River estuary (Zone1).

A new term was also added to the traditional advection equation to improve the model accuracy in simulating the advection process. Addition of the second advection term was observed to increase the computational cost in the model by 15 %, and caused a significant change (approximately 67 %) in the predicted number of particles in one of the accumulation zones within the lower Saint John River estuary.

Some inconsistencies between model results for analytical tests and those for the real-world application (Saint John River model) warrant further investigation in the future. For example, the TVD2 scheme resulted in a higher error (assessed based on a comparison to RK4, the most accurate scheme) than the RK2 scheme in the analytical tests. However, TVD2 showed closer agreement than RK2 to RK4 in the Saint John River model, illustrating the need for field validation in the future. Further improvement and development of CaMPSim-3D is envisaged in the future, including: 1) integrating physio-chemical processes (e.g.
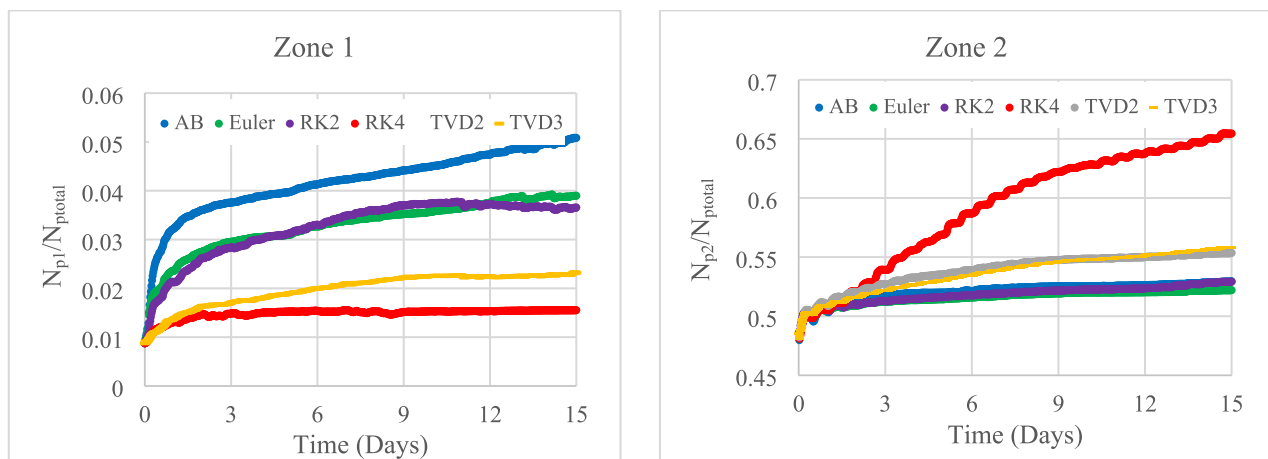

Fig. 9. Time series of particle counts (normalized by the total number of particles) in Zone 1 (Left), and Zone 2 (Right) predicted using different numerical schemes for Sc1.
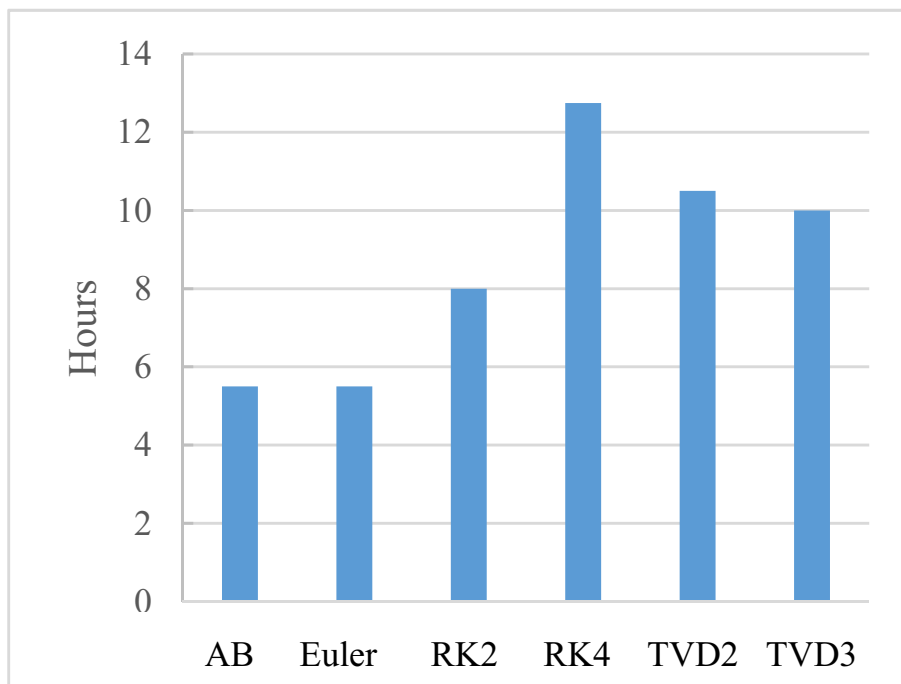
Fig. 10. Computation time for 500-time step PTM simulation of Sc1, using different advection schemes.
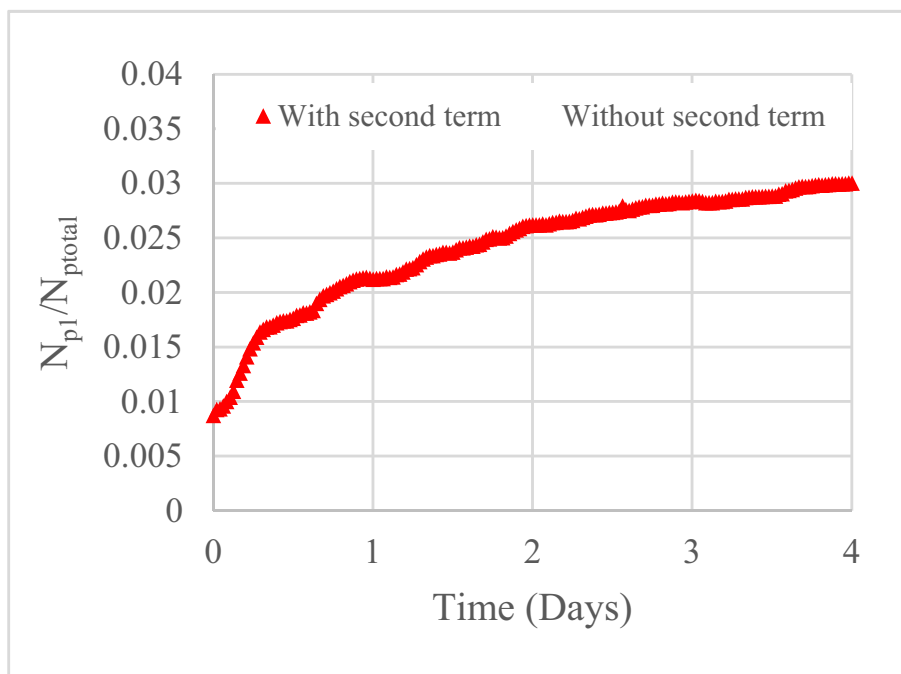

Fig. 11. Time series of particle counts (normalized by the total number of particles) in Zone 1 predicted for Sc1 using RK4 advection scheme with and without the second advection term.

degradation, weathering, biofilm growth, agglomeration); 2) integrating ice dynamics to driving transport processes influencing the transport of plastics such ice dynamics and; 3) adding back-tracing capabilities to the model to identify potential hotspots for accumulation, and sources of plastic pollution; 4) generalization of the model to further applications such as modeling oil spill, debris transport, surface drifters tracking; 5) parallelization of the model for CPU and GPU computations.

CRediT authorship contribution statement

Abolghasem Pilechi: Conceptualization, Methodology, Software, Validation, Formal analysis, Writing-Original draft preparation.
Abdolmajid Mohammadian: Methodology, Formal analysis, Writing-Reviewing and Editing.
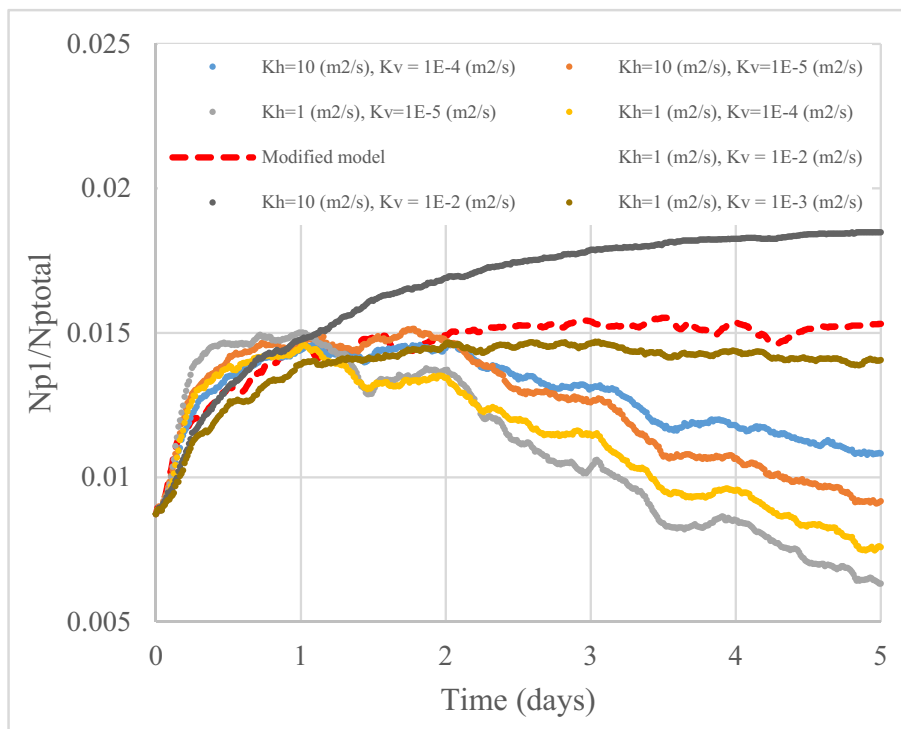Enda Murphy: Conceptualization, Writing- Reviewing and Editing.

Fig. 12. Time series of particle counts (normalized by the total number of particles) in Zone 1 predicted for Sc1 using the modified random walk model, and the naïve random walk model with different diffusivity coefficients.
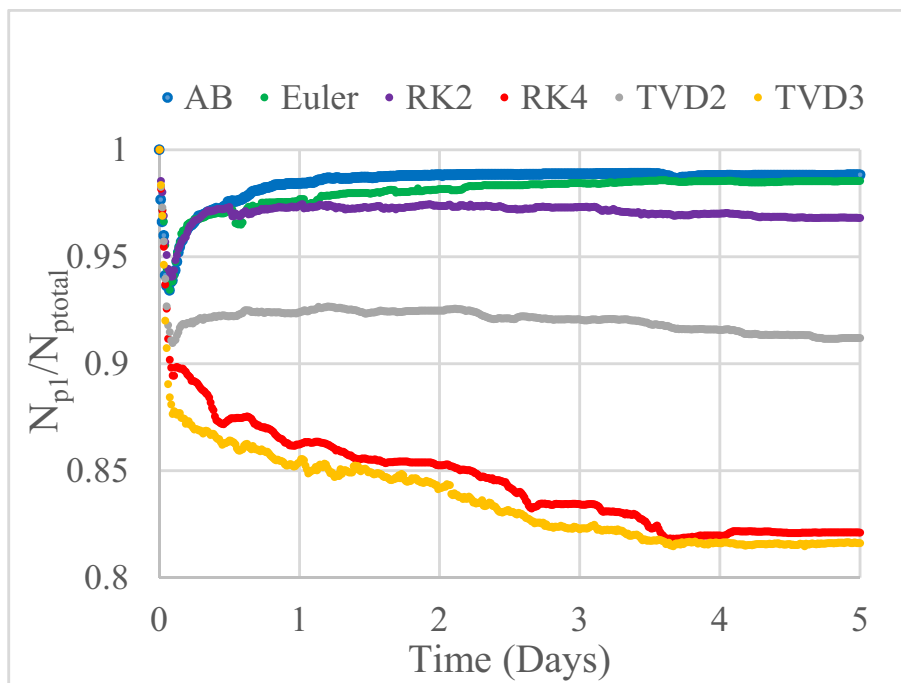

Fig. 13. Time series of number of particles (normalized by the total number of particles) in Zone 1 predicted using different advection schemes in Sc2.

Declaration of competing interest

The authors declare that they have no known competing financial interests or personal relationships that could have appeared to influence the work reported in this paper.

Data availability

Data will be made available on request.

References

Alosairi, Y., Al-Salem, S.M., Al Ragum, A., 2020. Three-dimensional numerical modelling of transport, fate and distribution of microplastics in the northwestern Arabian/ Persian gulf. Mar. Pollut. Bull. 161, 111723 https://doi.org/10.1016/j. marpolbul.2020.111723.

Andrady, Anthony L., 2011. Microplastics in the marine environment. Mar. Pollut. Bull. 1596–1605 https://doi.org/10.1016/j.marpolbul.2011.05.030.

Ashton, K., Holmes, L., Turner, A., 2010. In: Association of Metals With Plastic Production Pellets in the Marine Environment, pp. 2050–2055.

Barati, R., Neyshabouri, Seyed Ali Akbar Salehi, Ahmadi, Goodarz, 2018. Issues in eulerian-lagrangian modeling of sediment transport under saltation regime. Int. J. Sediment Res. 33, 441–461.

Barnes, D.K.A., Galgani, F., Thompson, R.C., Barlaz, M., 2009. Accumulation and fragmentation of plastic debris in global environments. Philosophical Transactions of the Royal Society B 1985–1998.

de Berg, M., Cheong, O., van Kreveld, M., Overmars, M., 2008. Computational Geometry. Springer, Berlin. https://doi.org/10.1007/978-3-540-77974-2.

Besseling, Ellen, Joris, T.K., Quik, MuzhiSun, Koelmans, Albert A., 2017. Fate of nano- and microplastic in freshwater systems: a modeling study. Environmental Pollution 540–548. https://doi.org/10.1016/j.envpol.2016.10.001.

Betts, Kellyn, 2008. Why small plastic particles may pose a big problem in the oceans. Environ. Sci. Technol. 8995 https://doi.org/10.1021/es802970v.

Bladé, E., Sánchez-Juny, M., 2016. Strategies in the 2D numerical modelling of wood transport in rivers. In: River Flow. Taylor & Francis, pp. 2333–2340.

Blanke, B., Raynaud, S., 1997. Kinematics of the Pacific Equatorial Undercurrent: An Eulerian and Lagrangian Approach from GCM Results. J. Phys. Oceanogr. 27 (6), 1038–1053. https://doi.org/10.1175/1520-0485(1997)027<1038:KOTPEU>2.0. CO;2.

Burchard, H., Bolding, K., 2002. GETM, a general estuarine transport model: scientific documentation. https://www.researchgate.net/publication/258128069_GETM _A_General_Estuarine_Transport_Model_Scientific_Documentation. (Accessed 19 September 2022).

Caruso, Gabriella, 2019. Microplastics as vectors of contaminants. Mar. Pollut. Bull. 146, 921–924. https://doi.org/10.1016/j.marpolbul.2019.07.052.

Chamas, Ali, Moon, Hyunjin, Zheng, Jiajia, Qiu, Yang, Tabassum, Tarnuma, Jang, Jun Hee, 2020. Degradation rates of plastics in the environment. ACS Sustainable Chem. Eng. 8, 3494–3511.

Chen, C., Zhao, N., Yue, T., Guo, J., 2015. Ageneralization of inverse distance weightin method via kernel regression and its application to surface modeling. Arab. J. Geosci. 8, 6623–6633.

Chubarenko, Irina, Zobkov, Mikhail Borisovich, Bagaev, Andrei, Esiukova, Elena, 2016. On some physical and dynamical properties of microplastic particles in marine environment. Mar. Pollut. Bull. 108 (1–2), 105–112. https://doi.org/10.1016/j. marpolbul.2016.04.048.

Cole, Matthew, Lindeque, Pennie, Halsband, Claudia, Galloway, Tamara S., 2011. Microplastics as contaminants in the marine environment: a review. Mar. Pollut. Bull. 62, 2588–2597.

Costa, M.F., Silva-Cavalcanti, J.S., Barbosa, C.C., Portugal, J.L., Barletta, M., 2011. Plastics buried in the inter-tidal plain of a tropical estuarine ecosystem. J. Coast. Res. 339–343.

Daily, Juliette, Matthew, Hoffman, J., 2020. Modeling the three-dimensional transport and distribution of multiple microplastic polymer types in Lake Erie. Marine Pollution Bulletin 154. https://doi.org/10.1016/j.marpolbul.2020.111024.

Dellino, P., Mele, D., Bonasia, R., Braia, G., La Volpe, L., Sulpizio, R., 2005. The analysis of the influence of pumice shape on its terminal. Geophys. Res. Lett. 32 (21) https:// doi.org/10.1029/2005GL023954.

Dimou, K.N., Adams, E.E., 1993. A random-walk, particle tracking model for well-mixed estuaries and coastal waters. Estuar. Coast. Shelf Sci. 37 (1), 99–110.

Dioguardi, F., Mele, D., Dellino, P., 2017. A new one-equation model of fluid drag for irregularly shaped particles valid over a wide range of Reynolds number. Journal of Geophysical Research: Solid Earth 144–156.

Fabbroni, Dott.ssa Nicoletta, 2009. Numerical Simulations of Passive Tracers Dispersion in the Sea. Università di Bologna, Bologna.

Goeury, C., Hervouet, J.-M., Baudin-Bizien, I., Thouvenel, F., 2014. A Lagrangian/ Eulerian oil spill model for continental waters. J. Hydraul. Res. 52, 36–48.

Gräwe, Ulf, Deleersnijder, Eric, Shah, Syed Hyder Ali Muttaqi, Heemink, Arnold Willem, 2012. Why the euler scheme in particle tracking is not enough: the shallow-sea pycnocline test case. Ocean Dyn. 62, 501–514.

ter Halle, Alexandra, Ladirat, Lucie, Gendre, Xavier, Goudouneche, Dominique, Pusineri, Claire, Routaboul, Corinne, Tenailleau, Christophe, Duployer, Benjamin, Perez, Emile, 2016. Understanding the fragmentation pattern of marine plastic debris. Environ. Sci. Technol. 50 (11), 5668–5675. https://doi.org/10.1021/acs. est.6b00594.

Hardesty, Britta D., Harari, Joseph, Isobe, Atsuhiko, Lebreton, Laurent, Maximenko, Nikolai, Potemra, Jim, Erik van Sebille, A., Vethaak, Dick,

Wilcox, Chris, 2017. Using numerical model simulations to improve the understanding of micro-plastic distribution and pathways in the marine environment. Front. Mar. Sci. 4, 9. https://doi.org/10.3389/fmars.2017.00030.

Herrera-Díaz, Israel E., Torres-Bejarano, Franklin M., Moreno-Martínez, Jatziri Y., Rodriguez-Cuevas, C., Couder-Castañeda, C., 2017. Light Particle Tracking Model for Simulating Bed Sediment Transport Load in River Areas. In: Mathematical Problems in Engineering. Hindawi.

Hervouet, J.-M., 2007. Hydrodynamics of Free Surface Flows, Modelling With the Finiter-Element Method. John Wiley & Sons Ltd, West Sussex.

van Hinsberg, M.A.T., ten Thije Boonkkamp, J.H.M., Toschi, F., Clercx, H.J.H., 2013. Optimal interpolation schemes for particle tracking in turbulence. Phys. Rev. E Stat. Nonlinear Soft Matter Phys. 4, 043307 https://doi.org/10.1103/ PhysRevE.87.043307.

Hoellein, Timothy J., Shogren, Arial J., Tank, Jennifer L., Risteca, Paul, Kelly, John J., 2019. Microplastic deposition velocity in streams follows patterns for naturally occurring allochthonous particles. Sci. Rep. 11 https://doi.org/10.1038/s41598-019-40126-3.

Hüffer, Thorsten, Praetorius, Antonia, Wagner, Stephan, von der Kammer, Frank, Hofmann, Thilo, 2017. Microplastic exposure assessment in aquatic environments: learning from similarities and differences to engineered nanoparticles. Environ. Sci. Technol. 2499–2507 https://doi.org/10.1021/acs.est.6b04054.

Hüffer, Thorsten, Praetorius, Antonia, Wagner, Stephan, von der Kammer, Frank, Hofmann, Thilo, 2017. Microplastic exposure assessment in aquatic environments. Environ. Sci. Technol. 2499–2507 https://doi.org/10.1021/acs.est.6b04054.

Hunter, J.R., 1987. Application of lagrangian particle-tracking techniques to modelling of dispersion in the sea. North-Holland Math. Stud. 145, 257–269.

Hunter, J.R., Craig, P.D., Phillips, H.E., 1993. On the use of random walk models with spatially variable diffusivity. J. Comput. Phys. 106, 366–376.

Isobe, Atsuhiko, Kubo, Kenta, Tamura, Yuka, Nakashima, Etsuko, Fujii, Naoki, Kako, Shinichio, 2014. Selective transport of microplastics and mesoplastics by drifting. Marine Pollution Bulletin 89, 324–330.

Israelsson, Peter H., Kim, Young Do, Eric Adams, E., 2006. A comparison of three Lagrangian approaches for extending near field mixing calculations. Environ. Model Softw. 21, 1631–1649.

Iwasakia, Shinsuke, Isobea, Atsuhiko, Kakob, Shinichiro, Uchidac, Keiichi, Tokaic, Tadashi, 2017. Fate of microplastics and mesoplastics carried by surface currents and wind waves: a numerical model approach in the sea of Japan. Mar. Pollut. Bull. 85–96 https://doi.org/10.1016/j.marpolbul.2017.05.057.

Jacob, Birgit, Partington, Jonathan R., Pott, Sandra, 2007. Interpolation by vector-valued analytic functions, with applications to controllability. J. Funct. Anal. 252, 514–549.

Jahnke, Annika, Hans, Peter H., Arp, Beate I., Escher, Berit Gewert, Gorokhova, Elena, Kühnel, Dana, Ogonowski, Martin, et al., 2017. Reducing uncertainty and confronting ignorance about the possible impacts of weathering plastic in the marine environment. Environ. Sci. Technol. Lett. 4, 85–90.

Jalón-Rojas, I., Wang, X.H., Fredj, E., 2019. A 3D numerical model to track marine plastic debris (TrackMPD): sensitivity of microplastic trajectories and fates to particle dynamical properties and physical processes. Marine pollution bulletin 141. https:// eia.nl/docs/mer/diversen/views_experiences_2012 p20-25.pdf.

Kaandorp, M.L.A., Dijkstra, H.A., van Sebille, E., 2020. Closing the Mediterranean Marine Floating Plastic Mass Budget: Inverse Modeling of Sources and Sinks. Environ. Sci. Technol. 54 (19), 11980–11989. https://doi.org/10.1021/acs. est.0c01984.

Kaiser, David, Kowalski, Nicole, Waniek, Joanna J., 2017. Effects of biofouling on the sinking behavior of microplastics. Environmental Research Letters 11. https://doi. org/10.1088/1748-9326/aa8e8b. IOP Publishing Ltd.

Kako, S.I., Isobe, A., Magome, S., Hinata, H., Seino, S., Kojima, A., 2011. Establishment of numerical beach-litter hindcast/forecast models: an application to Goto Islands, Japan. Mar. Pollut. Bull. 62 (2), 293–302.

Kelsey, Adrian, 1994. Modelling Particle Movement and Sediment Transport in Rivers. PhD Thesis. Lancaster University.

Khatmullina, Liliya, Chubarenko, Irina, 2019. Transport of marine microplastic particles: why is it so difficult to predict? Anthropocene Coasts 2, 293–305. https://doi.org/ 10.1139/anc-2018-0024.

Kirkpatrick, D.G., 1984. Optical search in planar subdivision. SIAM J. Comput. 12, 28–35.

Kjellsson, J., Döös, K., 2012. Lagrangian decomposition of the hadley and ferrel cells. Geophys. Res. Lett. 39, L15807. https://doi.org/10.1029/2012GL052420.

Koelmans, Albert A., Besseling, Ellen, Wegner, Anna, Foekema, Edwin M., 2013. Plastic as a carrier of POPs to aquatic organisms: model analysis. Environ. Sci. Technol. 47, 7812–7820. https://doi.org/10.1021/es401169n.

Kooi, Merel, van Nes, Egbert H., Scheffer, Marten, Koelmans, Albert A., 2017. Ups and downs in the ocean: effects of biofouling on vertical transport of microplastics. Environ. Sci. Technol. 7963–7971.

Lebreton, L.M., Greer, S.D., Borrero, J.C., 2012. Numerical modelling of floating debris in the world's oceans. Mar. Pollut. Bull. 64 (3), 653–661.

Lee, Jongmyoung, Hong, Sunwook, Song, Young Kyung, Hong, Sang Hee, Jang, Yong Chang, Jang, Mi, Heo, Nak Won, et al., 2013. Relationships among the abundances of plastic debris in different size classes on beaches in South Korea. Mar. Pollut. Bull. 349–354 https://doi.org/10.1016/j.marpolbul.2013.08.013.

Leet, C., Verley, P., Mullon, C., Parada, C., Brochier, T., Penven, P., Blanke, B., 2008. A lagrangian tool for modelling ichthyoplankton dynamics. Environ. Model. Softw 23, 1210–1214.

Li, Yandan, Li, Miao, ZhenLi, Lei Yang, Liu, Xiang, 2019. Effects of particle size and solution chemistry on triclosan sorption on polystyrene microplastic. Chemosphere 231, 308–314.

Li, Yanfang, Zhang, Hu.a., Tang, Cheng, 2020. A review of possible pathways of marine microplastics transport in the ocean. Anthropocene Coasts. https://doi.org/10.1139/anc-2018-0030.

Liubartseva, S., Coppini, G., Lecci, R., Clementi, E., 2018. Tracking plastics in the Mediterranean: 2D lagrangian model. Mar. Pollut. Bull. 151–162.

Liubartsevaa, S., Coppinib, G., Leccib, R., Clementic, E., 2018. Tracking plastics in the Mediterranean: 2D lagrangian model. Mar. Pollut. Bull. 129, 151–162.

Lo, Hoi-Shing, Xiaoyu, Xu., Wong, Chun-Yuen, Cheung, Siu Gin, 2018. Comparisons of microplastic pollution between mudflats and sandy beaches in Hong Kong. Environ. Pollut. 236, 208–217. https://doi.org/10.1016/j.envpol.2018.01.031.

Long, Marc, Moriceau, Brivaëla, Gallinari, Morgane, Lambert, Christophe, Huvet, Arnaud, Raffray, Jean, Soudant, Philippe, 2015. Interactions between microplastics and phytoplankton aggregates: impact on their respective fates. Mar. Chem. 175, 39–46. https://doi.org/10.1016/j.marchem.2015.04.003.

Macías, D., García-Gorriz, E., Stips, A., Cozar, A., Gonzalez-Fernandez, D., 2019. Surface Water Circulation Develops Seasonally Changing Patterns of Floating Litter Accumulation in the Mediterranean Sea. A Modelling Approach, 149.

Mansui, J., Molcard, A., Ourmières, Y., 2015. Modelling the transport and accumulation of floating marine debris in the Mediterranean basin. Mar. Pollut. Bull. 249–257.

Mansui, J., Darmon, G., Ballerini, T., van Canneyt, O., Ourmieres, Y., Miaudl, C., 2020. Predicting marine litter accumulation patterns in the Mediterranean basin: spatio-temporal variability and comparison with empirical data. Prog. Oceanogr. 182, 102268 https://doi.org/10.1016/j.pocean.2020.102268.

Michels, Jan, Stippkugel, Angela, Lenz, Mark, Wirtz, Kai, Engel, Anja, 2018. Rapid aggregation of biofilm-covered microplastics with marine biogenic particles. In: Proc. R. Soc. B, p. 9. https://doi.org/10.1098/rspb.2018.1203.

Mohammadian, A., Le Roux, D.Y., 2006. Int. J. Numer. Methods Fluids 52, 473–498.

Monsen, N.E., Cloern, J.E., Lucas, L.V., Monismith, S.G., 2002. A comment on the use of flushing time, residence time, and age as transport time scales. Limnol. Oceanogr. 47 (5), 1545–1553.

Moulinec, C., Denis, C., Pham, C.T., Rougé, D., Hervouet, J.M., Razafindrakoto, E., Barber, R.W., Emerson, D.R., Gu, X.J., 2011. TELEMAC: an efficient hydrodynamics suite for massively parallel architectures. Comput. Fluids 51 (1), 30–34. https://doi.org/10.1016/j.compfluid.2011.07.003.

Nandakumar, S., 2021. Particle Tracking of Microplastics in Aquatic Environments. Chalmers University of Technology, Gothenburg thesis.

Mountford, A.S., Morales Maqueda, M.A., 2021. Modeling the accumulation and transport of microplastics by sea ice. J. Geophys. Res. Oceans 126, e2020JC016826. https://doi.org/10.1029/2020JC016826.

Neuman, S.P., 1984. Adaptive Eulerian-Lagrangian finite element method for advection-dispersion. Int. J. Numer. Methods Eng. 321–397 https://doi.org/10.1002/nme.1620200211.

Nizzetto, Luca, Bussi, Gianbattista, Futter, Martyn N., Butterfielda, Dan, Whitehead, Paul G., 2016. A theoretical assessment of microplastic transport in river catchments and their retention by soils and river sediments. Environ. Sci.: Processes Impacts 18, 1050–1059. https://doi.org/10.1039/c6em00206d.

North, E.W., Adams, E.E., Schlag, Z., Sherwood, C.R., He, R., Hyun, K.H., Socolofsky, S. A., 2011. Simulating oil droplet dispersal from the Deepwater Horizon spill with a Lagrangian approach. Geophys. Monogr. Ser. 195, 217–226.

Oliveira, Anabela, Baptista, António M., 1995. A comparison of integration and interpolation Eulerian-Lagrangian methods. Int. J. Numer. Methods Fluids 21, 183–204. https://doi.org/10.1002/fld.1650210302.

Onink, Victor, Wichmann, David, Delandmeter, Philippe, van Sebille, Erik, 2019. The role of ekman currents, geostrophy, and stokes drift in the accumulation of floating microplastic. J. Geophys. Res. Oceans 124, 1474–1490. https://doi.org/10.1029/2018JC014547.

Politikos, D.V., Ioakeimidis, C., Papatheodorou, G., Tsiaras, K., 2017. In: Modeling the Fate and Distribution of Floating Litter Particles in the Aegean Sea (E. Mediterranean), 4, p. 191.

Potemra, James T., 2012. Numerical modeling with application to tracking marine debris. Mar. Pollut. Bull. 42–50 https://doi.org/10.1016/j.marpolbul.2011.06.026.

Preparata, Franco P., Tamassia, Roberto, 1992. Efficient point location in a convex spatial cell-complex. SIAM J. Comput. 267–280 https://doi.org/10.1137/0221020.

Quik, Joris T.K., van De Meent, Dik, Koelmans, Albert A., 2014. Simplifying modeling of nanoparticle aggregation sedimentation behavior in environmental systems: a theoretical analysis. Water Res. 193–201 https://doi.org/10.1016/j.watres.2014.05.048.

Rios, L.M., Moore, C., Jones, P.R., 2007. Persistent organic pollutants carried by synthetic polymers in the ocean environment. Mar. Pollut. Bull. 1230–1237.

Ruiz-Villanueva, V., Bladé-Castellet, E., Sánchez-Juny, M., Martí, B., Díez-Herrero, A., Bodoque, J.M., 2014. Two dimensional numerical modelling of wood transport. J. Hydroinform 16, 1077–1096.

Rummel, Christoph D., Jahnke, Annika, Gorokhova, Elena, Kühnel, Dana, Schmitt-Jansen, Mechthild, 2017. Impacts of biofilm formation on the fate and potential effects of microplastic in the aquatic environment. Environ. Sci. Technol. Lett. 4, 258–267. https://doi.org/10.1021/acs.estlett.7b00164.

Salamon, Peter, Fernàndez-Garcia, Daniel, Jaime Gómez-Hernández, J., 2006. A review and numerical assessment of the random walk particle tracking method. J. Contam. Hydrol. 87, 277–305. https://doi.org/10.1016/j.jconhyd.2006.05.005.

van Sebille, Erik, Griffies, Stephen M., Abernathey, Ryan, Adams, Thomas P., Berloff, Pavel, Biastoch, Arne, Blanke, Bruno, et al., 2018. Lagrangian ocean analysis: fundamentals and practices. Ocean Model. 121, 49–75. https://doi.org/10.1016/j.ocemod.2017.11.008.

Soto-Navarro, J., Jordá, G., Deudero, S., Alomar, C., Amores, Á., Compa, M., 2020. 3D hotspots of marine litter in the Mediterranean: a modeling study. Mar. Pollut. Bull. 155, 111159 https://doi.org/10.1016/j.marpolbul.2020.111159.

Spaulding, M.L., 2017. State of the art review and future directions in oil spill modeling. Mar. Pollut. Bull. 115, 7–19.

Staniforth, A., Cote, J., 1991. Semi-lagrangian transport schemes for atmospheric models—a review. Mon. Weather Rev. 2206–2223.

Strang, Gilbert, 2016. Calculus Volume 3. Massachusetts Institute of Technology, Massachusetts.

Szymczak, P., Ladd, A.J.C., 2003. Boundary conditions for stochastic solutions of the convection-diffusion equation. Phys. Rev. E 68 (3), 036704. https://doi.org/10.1103/PhysRevE.68.036704.

Van Melkebeke, M., Janssen, C., De Meester, S., 2020. Characteristics and sinking behavior of typical microplastics including the potential effect of biofouling : implications for remediation. Environ. Sci. Technol. 54 (14), 8668–8680. https://doi.org/10.1021/acs.est.9b07378.

Visser, Andre W., 1997. Using random walk models to simulate the vertical distribution of particles in a turbulent water column. Mar. Ecol. Prog. Ser. 158, 275–281.

Vouk, Ivana, Murphy, Enda, Church, Ian, Pilechi, Abolghasem, Cornett, Andrew, 2019. Three Dimensional Modelling of Hydrodynamics and Thermosaline Circulation in the Saint John River Estuary Canada. IAHR World Congress, Panama.

Waldschläger, Kryss, Schüttrumpf, Holger, 2019. Effects of particle properties on the settling and rise velocities of microplastics in freshwater under laboratory conditions. Environ. Sci. Technol. 53, 1958–1966. https://doi.org/10.1021/acs.est.8b06794.

Weinstein, John E., Crocker, Brittany K., Gray, Austin D., 2016. From macroplastic to microplastic: degradation of high-density polyethylene, polypropylene, and polystyrene in a salt marsh habitat. Environ. Toxicol. Chem. 35 (7), 1632–1640. https://doi.org/10.1002/etc.3432.

Wolk, Frank, 2003. Three-dimensional Lagrangian Tracer Modelling in Wadden Sea Areas. Diploma Thesis. Carl von Ossietzky University Oldenburg, Hamburg.

Wright, Stephanie L., Thompson, Richard C., Galloway, Tamara S., 2018. The physical impacts of microplastics on marine organisms: a review. Environ. Pollut. 178, 483–492. https://doi.org/10.1016/j.envpol.2013.02.031.

Wu, Fangzhu, Wang, Youji, Leung, Jonathan Y.S., Huang, Wei, Zeng, Jiangning, Tang, Yanbin, Chen, Jianfang, et al., 2020. Accumulation of microplastics in typical commercial aquatic species: A case study at a productive aquaculture site in China, 15 (708), 135432. https://doi.org/10.1016/j.scitotenv.2019.135432.

Xue, Pengfei, Schwab, David J., Zhou, Xing, Huang, Chenfu, Kibler, Ryan, Ye, Xinyu, 2018. A hybrid Lagrangian-Eulerian particle model for ecosystem simulation. J. Mar. Sci. Eng. 6 (4), 109. https://doi.org/10.3390/jmse6040109.

Yoon, J.H., Kawano, S., Igawa, S., 2010. Modeling of marine litter drift and beaching in the Japan Sea. Mar. Pollut. Bull. 60 (3), 448–463.

Zhang, Hua, 2017. Transport of microplastics in coastal seas. In: Estuarine, Coastal and Shelf Science. Elsevier, pp. 74–86. https://doi.org/10.1016/j.ecss.2017.09.032.

Zhang, Kai, Hamidian, Amir Hossein, Aleksandra Tubick, Yu., ZhangJames, K.H.Fang, Chenxi, Wu., Lam, Paul K.S., 2021. Understanding plastic degradation and microplastic formation in the environment: a review. Environmental Pollution 274, 116554. Elsevier.